



Cite this: *Nanoscale*, 2022, **14**, 16415

## Analytical separation techniques: toward achieving atomic precision in nanomaterials science

Krishnadas Kumaranchira Ramankutty\* and Thomas Bürgi  \*

The size- and shape-dependence of the properties are the most characteristic features of nanoscale matter. In many types of nanomaterials, there is a size regime wherein every atom counts. In order to fully realize the idea of '*maneuvering things atom by atom*' envisioned by Richard Feynman, synthesis and separation of nanoscale matter with atomic precision are essential. It is therefore not surprising that analytical separation techniques have contributed tremendously toward understanding the size- as well as shape-dependent properties of nanomaterials. Fascinating properties of nanomaterials would not have been explored without the use of these techniques. Here we discuss the pivotal role of analytical separation techniques in the progress of nanomaterials science. We begin with a brief overview of some of the key analytical separation techniques that are of tremendous importance in nanomaterials research. Then we describe how each of these techniques has contributed to the advancements in nanomaterials science taking some of the nanosystems as examples. We discuss the limitations and challenges of these techniques and future perspectives.

Received 22nd August 2022,  
Accepted 29th October 2022

DOI: 10.1039/d2nr04595h

[rsc.li/nanoscale](http://rsc.li/nanoscale)

### Introduction

Michael Faraday was one of the earliest who observed that 'divided forms' of matter exhibit strikingly new properties compared to that of bulk matter.<sup>1</sup> The horizon of nano-

materials has been expanding at a tremendous pace and a very large variety of nanomaterials emerged in the last few decades. The most important aspect of nanoscale matter is the size- and shape-dependence of their properties. Extremely high size- and shape-monodispersity and purity are essential for obtaining meaningful information of the properties of nanomaterials. Most of the synthesis routes, irrespective of the type of the nanomaterial, are inadequate to provide monodisperse

Department of Physical Chemistry, University of Geneva, 1211 Geneva 4, Switzerland. E-mail: [krdasnandipulam@gmail.com](mailto:krdasnandipulam@gmail.com), [thomas.buerghi@unige.ch](mailto:thomas.buerghi@unige.ch)



**Krishnadas Kumaranchira Ramankutty**

alloy precision metal clusters. He joined the lab of Prof. T. Bürgi at the University of Geneva, as a postdoc in 2017 where he studied optical and vibrational spectra of metal clusters. Since November 2021 he is a postdoc at the Biomolecular Nanotechnology Lab at CIC biomagUNE.

*Krishnadas Kumaranchira Ramankutty studied chemistry at the St Thomas' College, Thrissur, University of Calicut, Kerala, India (Bachelor) and obtained a master in applied chemistry from Cochin University of Science and Technology (CUSAT), Cochin, India. He obtained his PhD in 2016 from the Indian Institute of Technology Madras, Chennai, India, where he was working with Prof. T. Pradeep on atomic-*



**Thomas Bürgi**

*Thomas Bürgi studied chemistry and obtained his PhD (1995) at the University of Berne (Switzerland). After a postdoc at MIT, he did his habilitation at ETH, Zürich. He became assistant professor at the University of Neuchâtel (Switzerland, 2005) and full professor at the University of Heidelberg (2008). In 2010 he moved to the University of Geneva, where he is professor of physical chemistry. His research focuses on fundamental aspects and applications of chiral metal clusters and the development of in situ and chiroptical spectroscopy.*



and highly pure products. This necessitates the use of techniques for efficient size- and shape-dependent separation of nanoscale materials. The advances in almost any branch of nanomaterials research, be it metal nanoparticles or clusters, carbon nanomaterials, quantum dots, *etc.*, are due to the application of suitable separation and purification techniques. Mass spectrometry has also contributed significantly to the understanding of precise compositions and properties of nanoscale matter in the gaseous phase.<sup>2</sup> Fascinating properties of many types of nanomaterials such as structure, chemical reactivity, magnetism, photoluminescence, chirality, *etc.*, would not have been observed without these techniques. Purity as well as monodispersity (in size and shape) is crucial for spectroscopy of nanomaterials but also for many technological applications.

Understanding the evolution of properties in materials as they grow from atoms or molecules to bulk condensed matter through atomically precise assemblies (also referred to as 'clusters') is an important goal of nanomaterials research. In this journey from atoms/molecules to bulk materials, new properties emerge. It is not surprising that atomic precision is essential in order to observe those new properties of materials. In order to fully explore properties of nanoscale matter, we need appropriate tools to achieve atomic precision in synthesis and characterization. This has been mostly evident in case of metal clusters (as we discuss later) where several fascinating properties such as photoluminescence, chirality, *etc.*, were observed. Atomically precise materials are also essential in order to realize cluster-assembled materials. Only more effort and new experiments can unveil the phenomena of atomic precision in other types of materials, similar to what we currently enjoy in the case of metal clusters. Recently, there has been a trend in nanomaterials research community toward achieving atomic precision or zero-dimensionality in many types of materials such as chalcogenide quantum dots,<sup>3–5</sup> perovskites<sup>6–8</sup> and two-dimensional (2D) materials,<sup>9</sup> *etc.*, which are traditionally investigated in the three-dimensional (3D) or extended network forms. The principal motive behind these efforts is to overcome the limitations imposed by their 3D/bulk nature, such as defects, phase boundaries, *etc.*, preserving their inherent properties.<sup>7</sup> Another immediate implication of these attempts is to look for new properties emerging due to the atomic precision or low-dimensionality in these materials. This calls for achieving atomic precision in these low-dimensional materials which is closely related to the availability of potential separation techniques.

Here we discuss the pivotal role of analytical separation techniques in unveiling the fascinating size- as well as shape-dependent properties of nanomaterials. A brief overview of some of the key analytical separation techniques that are widely used in nanomaterials research is presented first. Then we discuss a few examples of nanomaterials and how separation techniques have been crucial in exploring their properties. We focus only on a few selected examples of nanomaterials in this article, however, challenges related to purity and monodispersity exist for almost any type of nanomaterials.

We finally summarize and provide a brief discussion on the limitations and challenges of these techniques and areas wherein further advancements are necessary, and also provide a future perspective. We believe that there are challenges to be addressed in the area of analytical separation tools toward an ambitious goal of achieving atomic precision in nanomaterials science.

## Analytical separation techniques in nanomaterials research: an overview

### Electrophoresis

Electrophoresis refers to the motion of dispersed particles or dissolved molecules in a fluid medium under the influence of an external electric field.<sup>10</sup> Charged particles or molecules move across the medium toward the electrodes of opposite polarity. The electrophoretic mobility of a molecule or particle depends on its size and charge. Investigations by Arne Tiselius in 1930s are considered to be the foundations of electrophoresis.<sup>11</sup> There are several variants for electrophoresis such as polyacrylamide gel electrophoresis (PAGE), agarose gel electrophoresis (AGE), capillary electrophoresis<sup>12,13</sup> (CE), *etc.* PAGE is traditionally used in biology for the separation of proteins, nucleic acids, *etc.* The stationary phase here is a gel prepared by polymerizing acrylamide using a free radical initiator such as ammonium persulfate (APS). Typically, acrylamide and bisacrylamide are mixed with a suitable buffer solution, APS and a stabilizer such as tetramethyl-ethylenediamine (TEMED). Bisacrylamide acts as a cross linker between the polymer chains formed from acrylamide. The relative concentrations of acrylamide, bisacrylamide, APS, TEMED are varied in order to get a gel with suitable pore sizes for the separation of the target analytes. After mixing the reagents, the solution is poured to the space between two vertically placed glass plates in a gel caster. Once the polymerization is finished, the gel can be used for electrophoresis. Once the separation is finished, the gel can be stained in order to see the separate bands that are formed. The gel can also be cut along the different bands and dispersed or dissolved in a suitable solvent in order to retrieve the separated analytes. PAGE and AGE are extremely useful technique for separation and purification of water-soluble (nano)materials. However, the quantities that can typically be separated by electrophoresis are rather small (mg) and the procedure can be time-consuming. CE is one of the techniques extensively used for separation of biological materials. However, this technique is only suitable for analytical purposes because only very small quantities can be separated due to the small size of the capillary tube. Electrophoretic separation of nanomaterials has been summarized in a review article by Surugau and Urban.<sup>14</sup>

### Liquid chromatography and associated techniques

Liquid chromatographic (LC) techniques such as high-pressure liquid chromatography (HPLC), liquid chromatography-mass



spectrometry (LC-MS), size exclusion chromatography (SEC), *etc.*, are extremely powerful in current research on metal nanosystems especially for atomically precise, ligand-protected metal clusters. The technique is based on the intermolecular interactions of the analyte and the stationary phase. LC has been used to size-separate atomically precise clusters and nanoparticles of noble metals. Chiral HPLC was used for the separation of enantiomers of atomically precise noble metal clusters.<sup>17</sup> LC-MS was used for the separation of structural isomers of thiolate-protected noble metal clusters in solution.<sup>18</sup> Some of these examples are presented in detail in a subsequent section. Note that many LC methods are mainly used as analytical tool but separation of small quantities (several mg) of material can be achieved using (semi-) preparative columns, although running many separation runs for achieving the desired quantities can be time-consuming. Since SEC is a widely used and a facile method to size-separate and purify a variety of nanomaterials, we discuss about this technique in some more detail below.

### Size exclusion chromatography (SEC)

SEC was discovered in 1955 by Grant Henry Lathe and Colin R. Ruthven.<sup>15,16</sup> They initially used starch as the stationary phase and later, materials such as agarose, acrylamide, *etc.*, were also used. Currently, a wide variety of materials are commercially available. Traditionally, SEC was used in biology and polymer research. Typically, a concentrated solution of the polydisperse sample is passed through the stationary phase, typically a long glass tube packed with the beads of the stationary phase. Sometimes, the beads of the stationary phase material need to be dispersed in a suitable solvent for a few hours prior to packing in the glass tube. During this process, the beads get swollen and pores of various sizes are formed. Larger particles elute faster than the smaller ones. As the solution containing the polydisperse sample passes through the stationary phase, larger molecules or particles cannot be trapped into the smaller pores and therefore, move faster through the stationary phase and elute first. The smaller molecules or particles are trapped into the pores of the stationary phase and hence, move slowly and elute later. The most important requirement for successful SEC is that the stationary phase should not lead to any irreversible adhesion or decomposition of the sample. If adsorption of the analyte on the SEC material can be neglected, the only parameter that determines the retention times (for a given stationary phase with a given pore size distribution) is the particle or molecular size. SEC is now widely used for the separation and purification of metal nanoparticles, clusters, quantum dots, nanocarbons, *etc.* The choice of the stationary phase, solvent, pH, *etc.*, vary depending on the nature of the sample. SEC is possible for a variety of materials including non-water-soluble materials and many SEC materials are commercially available. SEC is a cheap method, as it does not rely on expensive equipment, and it allows to separate relatively large quantities (tens of mg) in short time.

### Ultracentrifugation and centrifugal filtration

Ultracentrifugation is a technique for sedimentation of materials by centrifuging them at ultra-high speeds. This technique can be used for preparative or analytical purposes. This is one of the most essential and routine techniques in biology and materials sciences. Theodor Svedberg introduced ultracentrifugation technique and was awarded the Nobel prize in Chemistry in 1926 for his contributions in developing this technique.<sup>19</sup> Density gradient ultracentrifugation has been applied to separate various types of nanomaterials<sup>20</sup> and biological samples.<sup>21</sup> Here, the sample is centrifuged in a medium of graded density. This leads to better separation and less cross contamination between the fractions, but typically only small quantities can be separated. The commonly used media are iodixanol, sucrose, *etc.*

Centrifugal filtration is also one of the very important separation/purification techniques for nanomaterials. Centrifugal filter tubes with varying molecular weight cut offs (MWCO) are currently available on the market. These are used as the preliminary purification methods for removing excess of metal ions, ligands (such as thiols, DNA oligomers, *etc.*) and other small molecule residues after the synthesis.

### Separation using depletion forces

This is an interesting method of size- and shape-separation of colloidal systems utilizing entropic driving force<sup>22–25</sup> (see Fig. 2). This method has been used for several types of nanomaterials including plasmonic nanosystems, quantum dots, carbon nanotubes, *etc.* The basic idea of this technique is that an attractive force occurs between larger particles in a colloidal dispersion, depleting the amount of smaller particles between the larger ones. Because of the attraction between larger particles, they tend to aggregate and sediment, leaving the smaller particles in solution. In this final state, the entropy is higher because of the larger translational entropy of smaller particles gained by entering into the free solution (as opposed to the situation where the smaller ones are trapped between larger ones). Asakura and Oosawa were one of the first to demonstrate this phenomenon.<sup>22</sup>

### Size-selective precipitation

Size-selective precipitation is a highly useful method for the size-separation of various types of nanoparticles. This technique is based on the fact that nanoparticles can be precipitated from a solution by adding a non-solvent or bypassing pressurized gas. Nanoparticles (of different size, shape and composition) have different solubility and can therefore be separated (fractionated). This method has been used for narrowing the size-distribution of semiconductor nanoparticles and noble metal nanoparticles.<sup>26</sup> For example, Gravelsins *et al.* used this technique for Au nanoparticles that are soluble in organic solvents.<sup>26</sup>

### Dialysis

Dialysis is one of the membrane-based separation techniques used across diverse disciplines.<sup>27</sup> It is one of the simplest and



preliminary methods of separating various nanomaterials according to their molecular weights. This is routinely used for removing excess ligands, oligomeric metal-ligand complexes and sub-nanometer sized particles from metal nanomaterials.<sup>28–30</sup> Dialysis membranes of appropriate MWCOs are chosen depending on the type of material. Dialysis is typically performed for 2–3 days.

### Crystallization

Crystallization is an important technique to obtain highly pure samples from a complex mixture or from a reaction mixture.<sup>31</sup> Crystallization has also been used to obtain highly pure samples of atomically precise noble metal nanoclusters.<sup>63</sup> There is a growing interest to make colloidal nanocrystals of plasmonic metals,<sup>32,33</sup> chalcogenide quantum dots,<sup>34,35</sup> etc. Crystallization of colloidal systems is an extremely useful way to form their self-assembly,<sup>36</sup> superlattices, etc.

### Ion mobility mass spectrometry: size and shape separation in gaseous phase

Ion mobility mass spectrometry (IMS) is one of the techniques used for the size- and shape-dependent investigations of molecular properties in the gas phase. IMS was invented by Earl W. McDaniel in 1950s.<sup>37,38</sup> In 1960s, efforts to couple ion mobility measurements to mass spectrometers progressed. IMS separates gas phase ions depending on their drift times *i.e.*, the time they take to migrate through a buffer gas under an electric field.<sup>37</sup> Collision cross sections which depend on the size, shape and the charge of these ions can be calculated. Structural isomers possess different drift times as well as collision cross sections. This is referred to as drift-time ion mobility mass spectrometry (DTIMS). There are variants of IMS such as differential ion mobility mass spectrometry (DMS), aspiration ion mobility spectrometry (AIMS) and traveling-wave ion mobility spectrometry (TWIMS).<sup>37</sup> IMS is an extremely powerful tool for several practical applications such as detection of explosives, drugs and chemical warfare agents but also for nanomaterials. Advancements in this technique have been presented in recent reviews.<sup>39,40</sup>

### Interaction of nanomaterials with the separation devices

One of the hurdles in successful separation or purification of nanomaterials is the strong (sometimes irreversible) interaction between the samples and the active materials (stationary phases in SEC, HPLC, coating in centrifugation tubes, gels in PAGE, etc.) in the separation devices. This is especially important in case of plasmonic metal nanoparticles, atomically precise clusters, DNA-templated metal nanosystems, etc., wherein these materials tend to strongly adsorb onto the stationary phases in HPLC, SEC, etc. Sometimes, metal clusters also tend to react with the stationary phases leading to complete changes in size and composition. For example, Xie *et al.*, found that in the purification of ultrasmall thiolate-protected Ag nanoclusters *via* a desalting column and ultrafiltration, the nonluminescent Ag nanoclusters were spontaneously transformed to highly luminescent nanoclusters.<sup>41</sup> Alteration of

the charge states of metal clusters while passing them through a TLC plate is also reported. For example, for the facile conversion of anionic  $\text{Au}_{25}(\text{SR})_{18}$  ( $-\text{SR}$  is an alkyl/arylthiolate) to neutral  $\text{Au}_{25}(\text{SR})_{18}$ , TLC has been used.<sup>69</sup> Difficulties in recovering or redissolving the separated materials from the gels after PAGE is also a common problem encountered in gel chromatography. This occurs due to the irreversible binding of the samples with the gels. Another important factor is to use the solvents that are compatible with the separating devices. Advantages and disadvantages of some of the techniques discussed above are summarized in Table 1.

### The role of analytical separation techniques: a few examples

In the following discussion, we briefly mention how the techniques described above contributed to the understanding and advancements in the research on various types of nanomaterials.

### Carbon nanotubes

Carbon nanotubes (CNTs) can be considered as being formed by rolling a 2D layer of graphene along a specific direction. The chiral vector  $\vec{C}$  of a single-walled CNT (SWCNT) can be expressed as a function of graphene lattice vectors  $a_1$  and  $a_2$  with  $\vec{C} = n\vec{a}_1 + m\vec{a}_2$ . The structure of SWCNTs can therefore be described by the  $(n, m)$  indices. The properties of SWCNTs (conduction, optical chirality) depend strongly on their structure (and therefore on these indices). Even though synthesis routes have been advanced tremendously in the last decade, CNTs have been prepared in a polydisperse form, which requires further separation and purification in order to sort them according to their chirality indices. Techniques such as column chromatography, density gradient ultracentrifugation, etc., have contributed largely to the advancement of fundamentals and applications of CNTs.

Liu *et al.*, demonstrated that single-walled CNTs can be separated according to their sizes using column chromatography (see Fig. 1).<sup>42</sup> Ghosh *et al.*, showed that density gradient ultracentrifugation is extremely useful for sorting CNTs.<sup>43</sup> Depending on the indices of the SWCNTs, they can be metallic or semiconducting. Various methods have been adopted for separation these two types of SWCNTs.<sup>44</sup> One of the most fascinating properties of CNTs are their optical chirality.<sup>45</sup> However, samples prepared using standard procedures contain racemic mixtures of  $(n, m)$  SWCNTs. Using density gradient ultracentrifugation, enantiomers of  $(6, 5)$  SWCNTs were separated using chiral surfactants such as sodium cholate.<sup>43</sup> These surfactants adsorb differently on the two enantiomers of the tube, which is the basis for the successful enantiomeric separation. The separated enantiomers can be characterized by chiro-optical techniques, such as circular dichroism (CD) and Raman optical activity (ROA).<sup>46</sup> Fig. 3 shows the ROA spectra of the separated enantiomers of  $(6, 5)$  SWCNTs.

### Metal nanoparticles and atomically precise metal clusters

For metal nanomaterials, atomic precision has been achieved quite successfully. They present an example of success in



**Table 1** Summary of various analytical separation techniques used for nanomaterials and their advantages/disadvantages

Technique	Materials used for	Advantages/disadvantages
Dialysis	Metal nanoparticles, clusters, quantum dots, carbon dots, CNTs, etc.	Small to large scale, time consuming (a few hours to a few days)
Ultracentrifugation	Metal nanoparticles, quantum dots, carbon dots, CNTs, etc.	Small to large scale
Centrifugal filtration	Metal nanoparticles, clusters, quantum dots, carbon dots, CNTs, etc.	Small to large scale
SEC	Metal clusters, nanoparticles, carbon nanotubes, etc.	Small to large scale
Electrophoresis	Metal nanoparticles, clusters, DNA, etc.	Difficult to recover the separated bands, typically small scale
IMS	Metal clusters, proteins, DNA, etc.	Only gas phase, sample cannot be retrieved

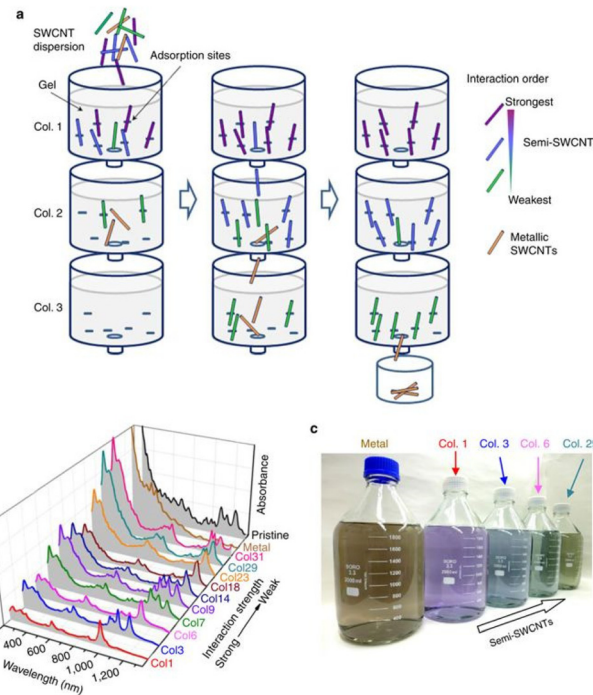


**Fig. 1** (a) Schematic diagram of single-surfactant multicolumn gel chromatography (SS-MUGEC) for separating SWCNTs. (b) Optical absorption spectra and (c) photograph of the separated metallic and semiconducting SWCNT fractions (2000 ml per fraction,  $\sim 0.8 \mu\text{g ml}^{-1}$ ). In b, the relative interaction strength between SWCNTs and the gel is indicated with an arrow (Col., column; Semi, semiconducting). This figure has been reproduced from ref. 42 with permission from Springer Nature, copyright 2011.

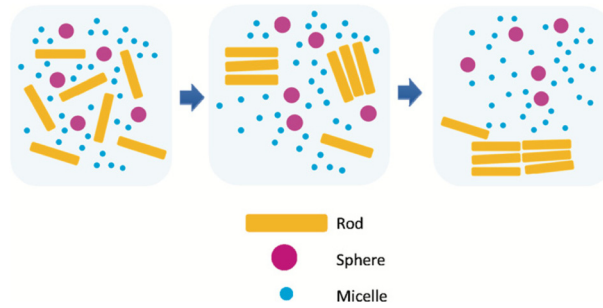


**Fig. 2** A schematic illustration of depletion-induced, entropy-driven separation of a multicomponent colloidal dispersion. Numerous, small micelles create an entropic, short-ranged attraction between the largest nanoparticles (yellow rods here). This results in preferential aggregation and sedimentation, leaving relatively smaller nanoparticles in solution. This figure has been reproduced with permission from ref. 25 with permission from the American Chemical Society, copyright 2010.

understanding the evolution of properties from atoms to atomically precise clusters and to larger bulk-like crystals. Synthesis of plasmonic metal nanoparticles, especially by wet chemical methods, results in a complex mixture, which is polydisperse in size as well as shape. Such a complex mixture can be separated according to the sizes and shapes of the nanoparticles

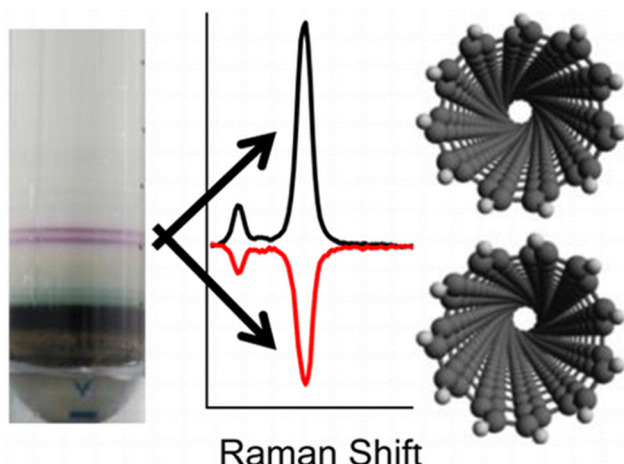


**Fig. 3** Resonance Raman optical activity spectra of enantiomers of (6, 5) carbon nanotubes. This figure has been reproduced from ref. 46 with permission from the American Chemical Society, copyright 2016.

using various techniques. Shape-dependent separation of quantum dots and noble metal nanosystems were achieved by using a variety of techniques such as PAGE, AGE,<sup>47</sup> ultracentrifugation,<sup>48</sup> SEC,<sup>49</sup> CE,<sup>50</sup> etc. For examples gold nanotriangles, rods and nanospheres can be separated from their mixture using agarose gel electrophoresis (see Fig. 4A–D).<sup>51</sup>

The field of atomically precise, molecule-like noble metal clusters has advanced tremendously in the last decade, thanks to the application of several analytical separation techniques. PAGE is one of the earliest separation techniques adapted to the field of ligand protected noble metal nanoparticles and clusters. This technique is limited to the separation of water-soluble clusters or particles. Several clusters such as

$\text{Au}_{25}(\text{SG})_{18}$ ,  $\text{Au}_{102}(\text{SR})_{44}$ , etc., have been separated from the crude mixtures. Some of the earliest attempts to use gel electrophoresis for metal nanosystems were reported by Whetten *et al.*, Arnaud *et al.*, and Parak *et al.*, in 2000, 2003 and 2005, respectively.<sup>52–54</sup> The first observation of chiroptical signatures in thiolate-protected noble metal clusters by Whetten *et al.*,<sup>52</sup> made use of PAGE. Kimura *et al.*, were the first to use PAGE for the size determination of gold nanoparticles in 2009.<sup>55</sup> They used glutathione-protected gold nanoparticles for the experiments. This technique is applicable for the separation and purification of protein-protected metal clusters as well.<sup>56</sup> The method is now widely used for the separation and purification of water-soluble metal nanoparticles and clusters.

SEC has played an immense role in the advancement of the metal nanoparticle research. In 1979, Henglein *et al.*, used SEC for the separation of CdS sols.<sup>57</sup> SEC has been used for the size and shape separation of nanoparticles since 1999.<sup>58,59</sup> SEC has been a valuable method for the isolation of atomically precise metal clusters from a crude mixture of polydisperse metal nanoparticles. For example, porous, styrene-divinylbenzene beads (brand name is Bio-Beads SX), are used for the separation of atomically precise noble metal clusters. SEC is capable of separating thiolate-protected noble metal clusters that differs in nuclearity by just two Au atoms as demonstrated by Knoppe *et al.* in case of  $\text{Au}_{38}$  and  $\text{Au}_{40}$ .<sup>60</sup> This is a fascinating example showcasing the power of SEC in metal cluster research. SEC is also important for the purification of these clusters. After preliminary solvent washes, the crude cluster mixture is passed through a SEC column to get rid of any free ligands, metal-ligand complexes and other residues in the reaction mixture. For all these reasons, SEC has now become a routine purification method to obtain clusters of high purity, especially for spectroscopic studies.

HPLC has been used for separating the enantiomers of atomically precise, ligand-protected noble metal clusters. Many ligand-protected noble metal clusters are in fact chiral.<sup>62</sup> The electron diffraction patterns of  $\text{Au}_{102}(\text{SR})_{24}$ , which was the first crystal structure to be resolved in the family of thiolate protected noble metal clusters, reveal the presence of enantiomers.<sup>63</sup> However, the separation of their enantiomers has not been possible for a long time. Crystal structure and theoretical calculations show that  $\text{Au}_{38}(\text{SR})_{24}$  is a chiral molecule.<sup>61,64</sup> Dolamic *et al.*, separated the enantiomers of this cluster using HPLC and it was the very first time in the family of thiolate protected noble metal clusters (see Fig. 5).<sup>61</sup>  $\text{Au}_{102}(\text{SR})_{24}$  and  $\text{Au}_{38}(\text{SR})_{24}$  are two beautiful examples demonstrating that these molecular clusters can be chiral even without any chiral components in them: chirality of these clusters arises due to the chiral arrangement of the ligands surrounding their metal cores.<sup>59–65</sup> Several new chiral clusters were synthesized and their chiroptical properties have been studied after successfully separating the enantiomers using HPLC.<sup>66,67</sup> Today, HPLC is the most frequently used techniques for the separation of the enantiomers of this type of clusters. Other techniques to separate enantiomers, like chiral phase transfer are also promising.<sup>68</sup>

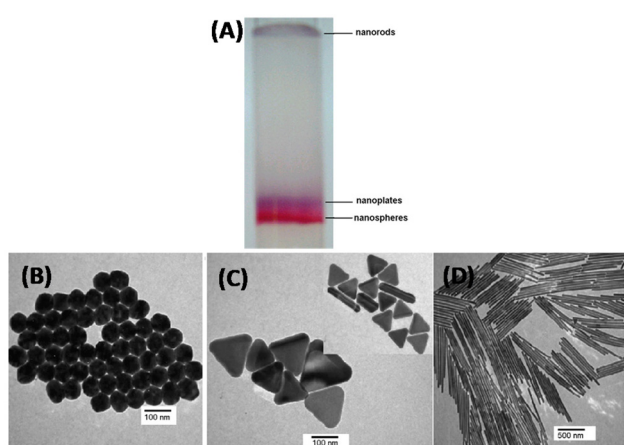


**Fig. 4** (A) Digital image of preparative agarose gel electrophoresis column shows the separated nanospheres (red band), nanoplates (blue band) and long nanorods (light brown band). TEM images of (B) separated pure nanospheres, (C) separated nanoplates (inset shows some short rods coexist with plates), and (D) purified long gold nanorods. This figure has been reproduced from ref. 50 with permission from Elsevier, copyright 2005.



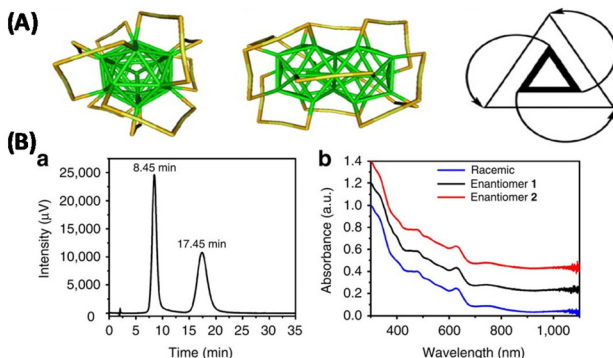


**Fig. 5** (A) Schematic showing the top view (left), side-view (middle) and a schematic representation highlighting the handedness of  $\text{Au}_{38}(\text{SCH}_2\text{CH}_2\text{Ph})_{24}$  (right). (B) HPLC-chromatogram (a) of the enantioseparation of rac- $\text{Au}_{38}(\text{SCH}_2\text{CH}_2\text{Ph})_{24}$  with the ultraviolet-visible detector at 380 nm. The peak at 8.45 min corresponds to enantiomer 1; the second peak at 17.45 min corresponds to enantiomer 2, and ultraviolet-visible spectra (b) of enantiomers 1 (black) and 2 (red) and of the racemate (blue). The spectra were normalized at 300 nm and off-set for clarity. The well-known ultra-violet-visible signature of  $\text{Au}_{38}$  is perfectly reproduced in all spectra, showing that the two collected fractions are composed of  $\text{Au}_{38}(\text{SCH}_2\text{CH}_2\text{Ph})_{24}$ . This figure has been reproduced from ref. 61 with permission from Springer Nature, copyright 2012.

Chirality arising from the achiral arrangement of metal atoms in the core is rather less explored. Recently, Whetten *et al.*, have used LC-MS for the separation of ligand protected noble metal clusters.<sup>18,68</sup> They further demonstrated the existence of structural isomers in  $\text{Ag}_{29}$  clusters in the liquid phase using LC-MS.<sup>17</sup>

Thin layer chromatography (TLC) is a routine technique in organic synthesis, but it has only recently been used in the field of ligand protected noble metal clusters. Ghosh *et al.*, has demonstrated for the first time that TLC can be employed as a simple and rapid tool for the separation and purification of metal clusters (see Fig. 6).<sup>69</sup> Their work showed that clusters

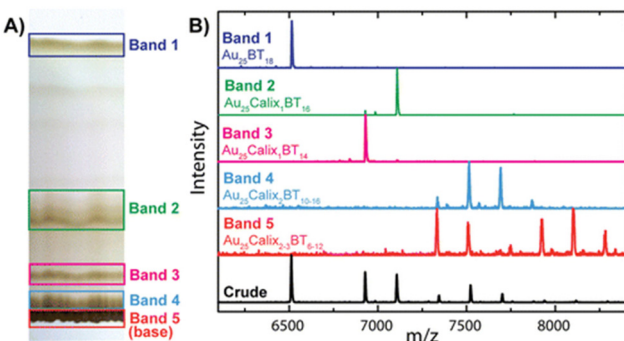


**Fig. 6** (A) Photograph of the TLC plate used for cluster separation. The faint bands observed between bands 1 and 2 are caused by sticking of the clusters to the TLC plate upon drying between runs. (B) MALDI MS data of  $\text{Au}_{25}\text{Calix}_{0-3}\text{BT}_{6-18}$  (Calix = Calixarene, BT = *n*-butanethiol) crude product before TLC (black trace) and bands 1–5 separated by TLC. This figure has been reproduced from ref. 69 with permission from the American Chemical Society, copyright 2014.

with mixed ligand composition can be separated according to their mode of binding (*i.e.*, monodentate *vs.* bidentate). Furthermore, they demonstrated that clusters such as  $\text{Au}_{25}(\text{BuS})_{18}$  and  $\text{Au}_{25}(\text{HT})_{18}$  (BuS and HT are 1-butanethiol and 1-hexanethiol, respectively) can also be separated using TLC. This technique has also been used in a few other cluster systems.<sup>70,71</sup> This is one of the easiest methods for separation and purification of clusters. Recently, Yan *et al.*, used TLC coupled with chemiluminescence for size determination and quantification of gold nanoparticles.<sup>72</sup>

HPLC has been used for separating the structural isomers in mixed ligand shell clusters resulting from the ligand exchange reactions. Sels *et al.*, have demonstrated that the isomers resulting from the exchange of the phenylethanethiolate (PET) with a dithiolate ligand, *i.e.*, *R/S*-1,1'-[binaphthylene]-2,2'-dithiol (BINAS), can be separated using HPLC.<sup>73</sup> A recent review by Negishi *et al.*, summarized the advancements in the HPLC in the field of thiolate protected atomically precise noble metal clusters.<sup>74</sup>

IMS has been used for the study of several types of bare gas phase species such as ionic clusters,<sup>75</sup> metal clusters, metal oxide clusters,<sup>76</sup> *etc.* There have been a few attempts to study the gas phase properties of ligand protected noble metal clusters also in the last decade. Dass *et al.*, conducted IMS measurements on the well-known  $\text{Au}_{25}(\text{SR})_{18}$ .<sup>77</sup> Bakshi *et al.*, identified structural isomers in the gas phase for  $\text{Ag}_{44}(\text{SR})_{30}$ .<sup>78</sup> They observed four distinct structural isomers of  $\text{Ag}_{44}(\text{FTP})_{30}^{4-}$  (FTP is 4-fluorothiophenol) (see Fig. 7). Recently, Hakkinen *et al.*, showed using IMS that the well-known  $\text{Au}_{25}(\text{SR})_{18}$  shows topological isomers in both anionic and cationic forms.<sup>79</sup> The topological isomerism of these clusters are assumed to be due to the rotation of the  $\text{Au}_{13}$  core of these clusters without break-

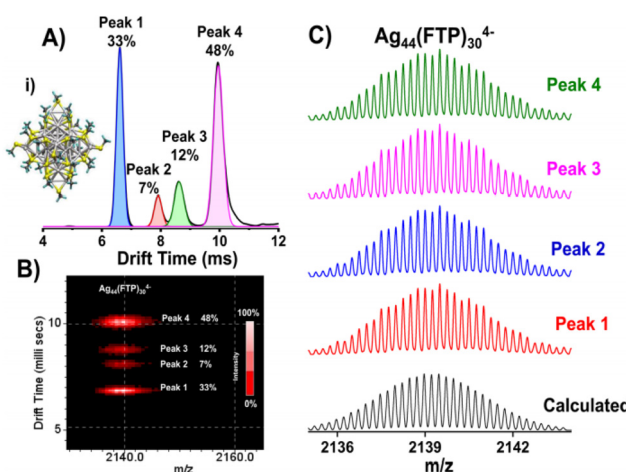


**Fig. 7** (A) Drift time profile of  $\text{Ag}_{44}(\text{FTP})_{30}^{4-}$  ( $m/z$  2140) showing four peaks due to distinct isomeric structures with relative abundances of 33, 7, 12, and 48%, respectively (calculated from peak area). Calculated structure of  $\text{Ag}_{44}(\text{SMe})_{30}$  is shown in inset (i). (B) Four well-defined spots observed in  $m/z$  vs. drift time plot. Each spot gave the same mass spectrum as shown in (C), matching with the calculated spectrum of the cluster. This figure has been reproduced from ref. 78 with permission from the American Chemical Society, copyright 2017.

ing any bonds in the metal–ligand interface.<sup>80</sup> Therefore, high resolution ion mobility mass spectrometry provides a way to unravel surprising dynamics of ligand-protected metal clusters.

### Towards achieving atomic precision in other materials

In this section we discuss how analytical separation techniques could be useful for making progress in achieving atomic precision or zero-dimensionality in materials such as chalcogenide quantum dots, zero-dimensional perovskites and various forms of molecular nanocarbons.

### Chalcogenide quantum dots

Quantum dots also have been prepared with a high polydispersity in size. There have been attempts to size-separate quantum dots using various techniques. Fujii *et al.*, for the first time, successfully separated Si quantum dots using polyacrylamide gel electrophoresis.<sup>81</sup> Song *et al.* used capillary gel electrophoresis for the separation of CdTe quantum dots.<sup>82</sup> High performance size exclusion chromatography (HPSEC) have also been used for the separation of Cd-based quantum dots.<sup>83</sup> Recently, Linkov *et al.*, used SEC for the purification of CdSe/ZnS quantum dots and their bioconjugates.<sup>84</sup>

There have been efforts to synthesize atomically precise chalcogenide quantum dots. Beecher *et al.*, investigated the transition from molecular vibrations to phonons in CdSe quantum dots using Raman spectroscopy.<sup>85</sup> Atomically precise QDs such as  $\text{Cd}_{35}\text{Se}_{20}\text{X}_{30}\text{L}_{30}$ ,  $\text{Cd}_{56}\text{Se}_{35}\text{X}_{42}\text{L}_{42}$ , and  $\text{Cd}_{84}\text{Se}_{56}\text{X}_{56}\text{L}_{56}$  were prepared for this purpose (see Fig. 8).

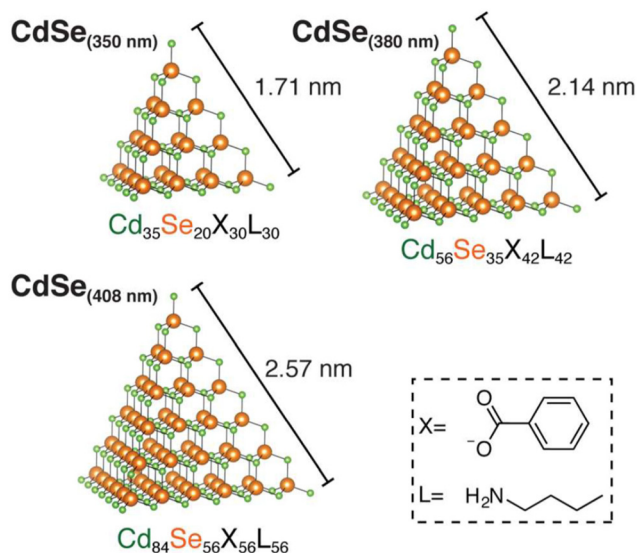


**Fig. 8** Three atomically precise, tetrahedral cadmium selenide QDs possessing known formulas and discrete dimensions with edge lengths ranging from 1.7 to 2.6 nm in size. The X and L type ligands are benzoate and *n*-butylamine, respectively. This figure has been reproduced from ref. 85 with permission from the American Chemical Society, copyright 2016.

Molecule-like silver-chalcogenide clusters such as  $[\text{Ag}_{34}\text{S}_3\text{SBB}_{20}(\text{CF}_3\text{COO})_6]^{2+}$  and  $\text{Ag}_{158}\text{S}_{79}(\text{SBB})_{32}$ , where SBB is 4-*tert*-butylbenzyl mercaptan were also synthesized.<sup>86,87</sup>

### Perovskites: quantum dots and zero-dimensional structures

A typical 3D metal halide perovskite has a general composition  $\text{ABX}_3$  wherein A is a monovalent cation ( $\text{Cs}^+$ ,  $\text{CH}_3\text{NH}_3^+$ , *etc.*), B is a bivalent metal ion ( $\text{Pb}^{2+}$ ,  $\text{Sn}^{2+}$ , *etc.*), and X is a halide ion ( $\text{Cl}^-$ ,  $\text{Br}^-$ ,  $\text{I}^-$ , *etc.*). Crystal structures of these perovskites consist of a 3D network of  $[\text{BX}_6]^{4-}$  octahedral units whose corners are connected. The metal cations occupy the octahedral voids. Photoexcitations produce excitons within the individual  $[\text{BX}_6]^{4-}$  octahedral units. The band gap and the optical properties of these materials depend upon the connectivity between the octahedral units. In a zero-dimensional perovskite (see Fig. 9), the individual octahedra are not shared at the corners and therefore, the optical properties largely reflect the properties of the individual octahedra (though they have large sizes).<sup>88</sup> In a perovskite quantum dot, the size of the particle is smaller than the exciton diameter. These materials are termed as perovskite QDs because they exhibit size-dependent band gaps and optical properties, just as metal chalcogenide quantum dots.<sup>89</sup> Umemoto *et al.*, recently showed that the monodispersity of perovskite QDs can be improved by Ostwald ripening in their colloidal solutions.<sup>89</sup>

### Graphene quantum dots

Graphene quantum dots (GQDs) are an emerging class of carbon nanomaterials. GQDs can be viewed as small pieces cut from a large, 2D sheet of graphene. GQDs are interesting because of their size- and shape-dependent properties and related applications.<sup>9,90</sup> For example, photoluminescence of GQDs has been attracting significant attention in the past few years.<sup>91,92</sup> Typically, synthesis of GQDs produces a complex mixture of GQDs that are highly polydisperse in terms of length, width and the number of layers. A variety of techniques such as dialysis,<sup>90</sup> size-selective precipitation,<sup>93</sup> gel column chromatography,<sup>92</sup> ultrafiltration,<sup>94</sup> *etc.*, have been used to

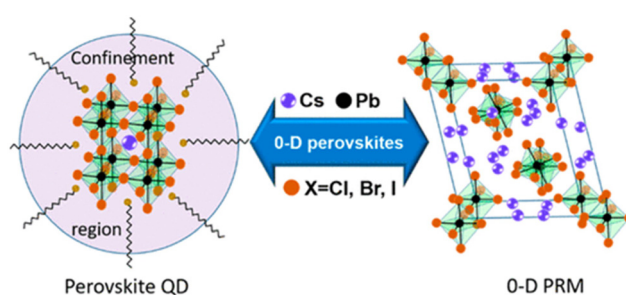


**Fig. 9** Schematic representation of two types of 0-D perovskites. Perovskite QDs with general formulas of  $\text{ABX}_3$  and size less than the exciton Bohr diameter (represented by the circle) and 0-D perovskite-related materials with spatially isolated octahedra in a bulk crystal lattice. This figure has been reproduced from ref. 88 with permission from the American Chemical Society, copyright 2018.



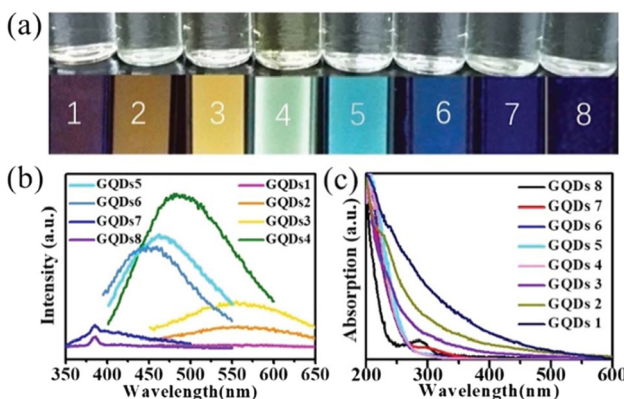


**Fig. 10** (a) The top row shows the optical images of aqueous suspensions of GQDs 1–8 obtained under daylight lamp; the bottom row shows the optical images of the aqueous suspensions of GQDs 1–8 acquired under UV/irradiation (302 nm) (GQDs-1/red, GQDs-2/orange, GQDs-3/yellow, GQDs-4/green, GQDs-5/cyan, GQDs-6/light blue, GQDs-7/blue, GQDs-8/purple). (b) PL spectra of GQDs 1–8 (the excitation wavelength is 340 nm). (c) UV-vis absorption spectra of GQDs 1–8 (the spectra were normalized at 200 nm for comparison). This figure has been reproduced from ref. 92 with permission from the Royal Society of Chemistry, copyright 2019.

size- and shape-separate as synthesized GQDs (Fig. 10). Xue *et al.*, used an amine-assisted chemical cutting method followed by ultrafiltration using membranes in order to produce nearly monodisperse GQDs with uniform lateral size and layer number.<sup>94</sup>

Mohanty *et al.*, developed a nanoscale cutting method (see Fig. 11) using a diamond tip for the production of GQDs of controllable sizes and shapes.<sup>95</sup> The advantage of this method is that GQDs with predetermined sizes and shapes can be cut

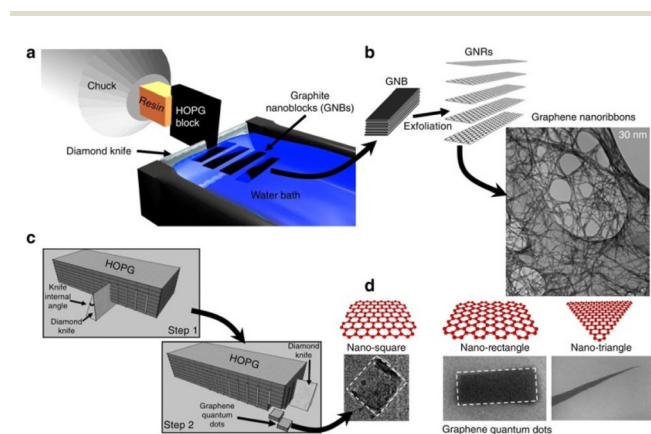


**Fig. 11** (a) A descriptive sketch of the nanotomy process showing the diamond-knife-based mechanical cleaving of HOPG block to produce GNBs for GNR production. (c) Sketch of the two-step nanotomy process to produce GNBs for GQD production. (b and d) GNRs and GQDs are produced by exfoliating the corresponding GNBs in chlorosulphonic acid (superacid). TEM micrographs of 30 nm GNRs and FESEM micrographs of GQDs of different shapes (square, rectangle and triangle). This figure has been reproduced from ref. 95 with permission from Springer Nature, copyright 2012.

from a block of HOPG by controlling the alignment of the diamond knife and the graphite block. Such particles within ~10–100 nm can be obtained at a size resolution of 5 nm.

### Carbon dots

Recently a class of materials called carbon dots have emerged with interesting properties such as strong photoluminescence, catalytic activity, chirality *etc.*<sup>96–99</sup> The structure and composition of such carbon-rich materials is ambiguous and the origin of their properties is not yet understood clearly. Various analytical separation techniques have been employed to purify as well as size-separate these materials which is necessary to unravel the mysteries behind the structure, composition and properties of these promising materials.

### DNA nanotechnology

Separation/purification techniques have played a tremendous role in the advancement of DNA nanotechnology. Various techniques, such as ultracentrifugation,<sup>100</sup> centrifugal filtration, gel chromatography, electrophoresis,<sup>101,102</sup> *etc.*, were employed for the initial purification of DNA nanostructures. These techniques are also routinely employed in the synthesis of DNA-nanohybrids with plasmonic nanosystems, quantum dots, fluorescent metal clusters, *etc.* Importance of such methods in DNA nanotechnology has been addressed in a review by Mathur and Medintz.<sup>103</sup>

## Summary and future aspects

Analytical separation techniques played a pivotal role in unveiling the fascinating size- and shape-dependent properties of nanomaterials. A few of these techniques have been briefly discussed and it was shown how the separation techniques contributed to the advancement of the field by presenting a few selected types of nanomaterials. The demand for more facile and efficient separation techniques with enhanced resolution is increasing as researchers aspire to achieve atomic precision in almost any type of nanomaterials.

Photophysical and photochemical investigations of many of the nanosystems have been carried out using samples with inadequate purity and poor monodispersity, and this can lead to wrong conclusions. For example, broad photoluminescence emission bands, occurrence of multiexponential luminescence lifetimes, *etc.*, in many fluorescent nanosystems (metal clusters, carbon dots) might be due to polydispersity and impurities.

Development of even more powerful separation techniques for atomically precise metal clusters will further boost the field. For example, techniques able to achieve separation with single atom-precision (for example, a technique that could separate  $\text{Au}_{25}(\text{SR})_{18}$  and  $\text{Au}_{24}(\text{SR})_{18}$ ) will be extremely useful.

Achieving atomic precision in the plasmonic size regimes remains a challenge. Better separation techniques could help in this regard to, at least, narrow down the polydispersity of plasmonic particles.



Water soluble nanomaterials are more difficult to separate compared to organic soluble materials. This is mostly due to the necessity to accurately control the pH, ionic strength, *etc.*, of the samples and due to the strong adhesion of particles to the separating medium. More facile techniques are required to address the challenges on water-soluble nanomaterials.

We may need to develop new materials to efficiently achieve such separation, for example, new types of stationary phase materials for size exclusion chromatography. These attempts could lead to 'atomic level sieving' which will be helpful toward achieving the ultimate goal of '*maneuvering things atom by atom*'.

Methods for faster, and large-scale separation of chiral metal nanoparticles, atomically precise clusters (chiral nanomaterials in general) are necessary as techniques such as HPLC (which is commonly used for these purposes) provide very small quantities of separated samples. Techniques such as chiral TLC separation could prove very useful in metal cluster chemistry.

We think that the investigations of biological effects and applications of nanomaterials need to be conducted with materials with better purity and monodispersity. We think that '*every atom counts*' effects in biology need to be more systematically investigated with size- as well as shape-controlled samples.

Atomic precision in materials such as quantum dots, graphene quantum dots and other molecular nanocarbons, *etc.*, is yet to be explored in this regard. The research on molecular nanocarbons also demands for the efficient size- as well as shape-based separation techniques.<sup>104</sup> We believe that just like metal nanosystems, molecular nanocarbon materials would exhibit fascinating size- and shape-dependent properties that could be discovered by preparing mono-disperse samples with the aid of advanced separation techniques.

We should keep in mind the possibility that even for a given type of nanomaterial, multiple techniques may be needed to ensure the purity and size- as well as shape-monodispersity. There will be challenges specific to a given class of nanomaterial in adopting separation techniques. We hope that this article could trigger efforts to develop new strategies for fast and efficient size- and shape-dependent separation of nanomaterials.

## Conflicts of interest

There are no conflicts to declare.

## Acknowledgements

The generous support by the University of Geneva and the Swiss National Science Foundation (grant number 200020\_19223) is kindly acknowledged.

## References

- 1 M. Faraday, X. The Bakerian Lecture, *Phil. Trans. R. Soc.*, 1857, **147**, 145–181.
- 2 P. Chakraborty and T. Pradeep, *NPG Asia Mater.*, 2019, **11**, 48.
- 3 W. Wegscheider, G. Schedelbeck, G. Abstreiter, M. Rother and M. Bichler, *Phys. Rev. Lett.*, 1997, **79**, 1917–1920.
- 4 C. Shi, A. N. Beecher, Y. Li, J. S. Owen, B. M. Leu, A. H. Said, M. Y. Hu and S. J. L. Billinge, *Phys. Rev. Lett.*, 2019, **122**, 026101.
- 5 A. N. Beecher, X. Yang, J. H. Palmer, A. L. LaGrassa, P. Juhas, S. J. L. Billinge and J. S. Owen, *J. Am. Chem. Soc.*, 2014, **136**, 10645–10653.
- 6 O. F. Mohammed, *J. Phys. Chem. Lett.*, 2019, **10**, 5886–5888.
- 7 J. Almutlaq, J. Yin, O. F. Mohammed and O. M. Bakr, *J. Phys. Chem. Lett.*, 2018, **9**, 4131–4138.
- 8 J. Yin, P. Maity, M. De Bastiani, I. Dursun, O. M. Bakr, J.-L. Brédas and O. F. Mohammed, *Sci. Adv.*, 2017, **3**, e1701793.
- 9 Z. Zhang, J. Zhang, N. Chen and L. Qu, *Energy Environ. Sci.*, 2012, **5**, 8869–8890.
- 10 R. Stringer, Electrophoresis: An Overview, in *Encyclopaedia of Analytical Science*, ed. R. Stringer, P. Worsfold, A. Townshend and C. Poole, Elsevier, Oxford, 2nd edn, 2005, pp. 356–363.
- 11 O. Vesterberg, *J. Chromatography*, 1989, **480**, 3–19.
- 12 A. Fekete and P. Schmitt-Kopplin, Capillary electrophoresis, in *Food Toxicants Analysis*, ed. Y. Picó, Elsevier, Amsterdam, 2007, ch. 15, pp. 561–597.
- 13 C. Fanali, G. D'Orazio and S. Fanali, Capillary electrophoresis-mass spectrometry: History, general principles, theoretical aspects, and state-of-the-art applications, in *Hyphenations of Capillary Chromatography with Mass Spectrometry*, ed. P. Q. Tranchida and L. Mondello, Elsevier, 2020, ch. 4, pp. 413–447.
- 14 N. Surugau and P. L. Urban, *J. Sep. Sci.*, 2009, **32**, 1889–1906.
- 15 G. H. Lathe and C. R. Ruthven, *Biochem. J.*, 1955, **60**, xxxiv.
- 16 G. H. Lathe and C. R. Ruthven, *Biochem. J.*, 1956, **62**, 665–674.
- 17 I. Dolamic, S. Knoppe, A. Dass and T. Bürgi, *Nat. Commun.*, 2012, **3**, 798.
- 18 D. M. Black, G. Robles, P. Lopez, S. B. H. Bach, M. Alvarez and R. L. Whetten, *Anal. Chem.*, 2018, **90**, 2010–2017.
- 19 J. W. Williams, K. E. Van Holde, R. L. Baldwin and H. Fujita, *Chem. Rev.*, 1958, **58**, 715–744.
- 20 P. Li, J. Huang, L. Luo, Y. Kuang and X. Sun, *Anal. Chem.*, 2016, **88**, 8495–8501.
- 21 J. D. Robertson, L. Rizello, M. Avila-Olias, J. Gaitzsch, C. Contini, M. S. Magon, S. A. Renshaw and G. Battaglia, *Sci. Rep.*, 2016, **6**, 27494.
- 22 S. Asakura and F. Oosawa, *J. Chem. Phys.*, 1954, **22**, 1255–1256.
- 23 T. G. Mason, *Phys. Rev. E: Stat., Nonlinear, Soft Matter Phys.*, 2002, **66**(6), 4.



24 M. Adams, Z. Dogic, S. L. Keller and S. Fraden, *Nature*, 1998, **393**, 349–352.

25 K. Park, H. Koerner and R. A. Vaia, *Nano Lett.*, 2010, **10**, 1433–1439.

26 S. Gravelsins and A.-A. Dhirani, *RSC Adv.*, 2017, **7**, 55830–55834.

27 N. Wu, Y. Wyart, Y. Liu, J. Rose and P. Moulin, *Environ. Tech. Rev.*, 2013, **2**, 55–70.

28 R. L. Spina, V. Spampinato, D. Gilliland, I. Ojea-Jimenez and G. Ceccone, *Biointerphases*, 2017, **12**, 031003.

29 Y. Cao, V. Fung, Q. Yao, T. Chen, S. Zang, D. Jiang and J. Xie, *Nat. Commun.*, 2020, **11**, 5498.

30 H. Huang, G. B. Hwang, G. Wu, K. Karu, H. D. Toit, H. Wu, J. Callison, I. P. Parkin and A. Gavriilidis, *Chem. Eng. J.*, 2020, **383**, 123176.

31 H. J. M. Cramer and G. M. V. Rosmalen, *Encyclopedia of Separation Science*, 2000, pp. 64–84.

32 M. Baginzky, A. Pedraso-Tardajos, T. Atlantzis, M. Tupikowska, A. Vetter, E. Tomczyk, R. N. S. Suryadharma, M. Pawlak, A. Andruszkiewicz, E. Gorecka, D. Pociecha, C. Rockstuhl, S. Bals and W. Lewandowski, *ACS Nano*, 2021, **15**, 4916–4926.

33 D. Nykypanchuk, M. A. Maye, D. van der Lelie and O. Gang, *Nature*, 2008, **451**, 549–552.

34 F. Bertolotti, D. N. Dirin, M. Ibanez, F. Krumeich, A. Cervellino, R. Frison, O. Voznyy, E. H. Sargent, M. V. Kovalenko, A. Gugliardi and N. Masciocchi, *Nat. Mater.*, 2016, **15**, 987–994.

35 N. Zheng, X. Bu, H. Lu, Q. Zhang, P. Feng and J. Am, *Chem. Soc.*, 2005, **127**, 11963–11965.

36 M. Grzelczak, J. Vermant, E. M. Furst and L. M. Liz-Marzan, *ACS Nano*, 2010, **4**, 3591–3605.

37 A. B. Kanu, P. Dwivedi, M. Tam, L. Matz and H. H. Hill Jr., *J. Mass Spectrom.*, 2008, **43**, 1–22.

38 E. W. McDaniel, D. W. Martin and W. S. Barnes, *Rev. Sci. Instrum.*, 1962, **33**, 2–7.

39 R. Cumeras, E. Figueras, C. E. Davis, J. I. Baumbach and I. Gràcia, *Analyst*, 2015, **140**, 1376–1390.

40 R. Cumeras, E. Figueras, C. E. Davis, J. I. Baumbach and I. Gràcia, *Analyst*, 2015, **140**, 1391–1410.

41 X. Yuan, Q. Yao, Y. Yu, Z. Luo, X. Dou and J. Xie, *J. Phys. Chem. Lett.*, 2013, **4**, 1811–1815.

42 H. Liu, D. Nishide, T. Tanaka and H. Kataura, *Nat. Commun.*, 2011, **2**, 309.

43 S. Ghosh, S. M. Bachilo and R. B. Weisman, *Nat. Nanotechnol.*, 2010, **5**, 443–450.

44 R. Krupke, F. Hennrich, H. V. Löhneysen and M. M. Kappes, *Science*, 2003, **301**, 344–347.

45 X. Wei, T. Tanaka, T. Hirakawa, M. Tsuzuki, G. Wang, Y. Yomogida, A. Hirano and H. Kataura, *Carbon*, 2018, **132**, 1–7.

46 M. Magg, Y. Kadria-Vili, P. Oulevey, R. B. Weisman and T. Bürgi, *J. Phys. Chem. Lett.*, 2016, **7**, 221–225.

47 M. Hanauer, S. Pierrat, I. Zins, A. Lotz and C. Sönnichsen, *Nano Lett.*, 2007, **7**, 2881–2885.

48 V. Sharma, K. Park and M. Srinivasarao, *Proc. Natl. Acad. Sci. U. S. A.*, 2009, **106**, 4981–4985.

49 L. Pitkänen and A. M. Striegel, Size-exclusion chromatography of metal nanoparticles and quantum dots, *TrAC, Trends Anal. Chem.*, 2016, **80**, 311–320.

50 F.-K. Liu, F.-H. Ko, P.-W. Huang, C.-H. Wu and T.-C. Chu, *J. Chromatogr. A*, 2005, **1062**, 139–145.

51 X. Xu, K. K. Caswell, E. Tucker, S. Kabisatpathy, K. L. Brodhacker and W. Scrivens, *J. Chromatogr. A*, 2007, **1167**, 35–41.

52 T. G. Schaff and R. L. Whetten, *J. Phys. Chem. B*, 2000, **104**, 2630–2641.

53 I. Arnaud, J.-P. Abid, C. Roussel and H. H. Girault, *Chem. Commun.*, 2005, 787–788.

54 W. J. Parak, T. Pellegrino, C. M. Michelet, D. Gerion, S. C. Williams and A. P. Alivisatos, *Nano Lett.*, 2003, **3**, 33–36.

55 K. Kimura, N. Sugimoto, S. Sato, H. Yao, Y. Negishi and T. Tsukuda, *J. Phys. Chem. C*, 2009, **113**, 14076–14082.

56 M. Kluz, H. Nieznańska, R. Dec, I. Dziećielewski, B. Niżyński, G. Ścibisz, W. Puławski, G. Staszczak, E. Klein, J. Smalc-Koziorowska and W. Dzwolak, *PLoS One*, 2019, **14**, e0218975.

57 Ch.-H. Fischer, J. Lilie, H. Weller, L. Katsikas and A. Henglein, Photochemistry of colloidal semiconductors. 29. Fractionation of CdS sols of small particles by exclusion chromatography, *Ber. Bunsen-Ges. Phys. Chem.*, 1989, **93**, 61–64.

58 G.-T. Wei, F.-K. Liu and C. R. C. Wang, *Anal. Chem.*, 1999, **71**, 2085–2091.

59 G.-T. Wei and F.-K. Liu, *J. Chromatogr. A*, 1999, **836**, 253–260.

60 S. Knoppe, J. Boudon, I. Dolamic, A. Dass and T. Bürgi, *Anal. Chem.*, 2011, **83**, 5056.

61 I. Dolamic, S. Knoppe, A. Dass and T. Bürgi, *Nat. Commun.*, 2012, **3**, 798.

62 J.-H. Huang, X.-Y. Dong, Y.-J. Wang and S.-Q. Zhang, *Coord. Chem. Rev.*, 2022, **470**, 214729.

63 P. D. Jadzinsky, G. Calero, C. J. Ackerson, D. A. Bushnell and R. D. Kornberg, *Science*, 2007, **318**, 430–433.

64 I. Dolamic, B. Varnholt and T. Bürgi, *Nat. Commun.*, 2015, **6**, 7117.

65 H. Yoshida, M. Ehara, U. D. Priyakumar, T. Kawai and T. Nakashima, *Chem. Sci.*, 2020, **11**, 2394–2400.

66 S. Knoppe, I. Dolamic, A. Dass and T. Bürgi, *Angew. Chem. Int. Ed.*, 2012, **51**, 7589–7591.

67 D. M. Black, G. Robles, S. B. H. Bach and R. L. Whetten, *Ind. Eng. Chem. Res.*, 2018, **57**, 5378–5384.

68 S. Knoppe, O. S. Wong, S. Malola, H. Hakkinen, T. Bürgi, T. Verbiest and C. J. Ackerson, *J. Am. Chem. Soc.*, 2014, **136**, 4129.

69 A. Ghosh, J. Hassinen, P. Pulkkinen, H. Tenhu, R. H. A. Ras and T. Pradeep, *Anal. Chem.*, 2014, **86**, 12185–12190.

70 A. Mathew, E. Varghese, S. Choudhury, S. K. Pal and T. Pradeep, *Nanoscale*, 2015, **7**, 14305–14315.



71 S. Bhat, A. Baksi, S. K. Mudedla, G. Natarajan, V. Subramanian and T. Pradeep, *J. Phys. Chem. Lett.*, 2017, **8**, 2787–2793.

72 N. Yan, Z. Zhu, D. He, L. Jin, H. Zheng and S. Hu, *Sci. Rep.*, 2016, **6**, 24577.

73 S. Sels, N. Barrabes, S. Knoppe and T. Bürgi, *Nanoscale*, 2016, 11130.

74 Y. Negishi, S. Hashimoto, A. Ebina, K. Hamada, S. Hossain and T. Kawakami, *Nanoscale*, 2020, **12**, 8017–8039.

75 K. Ohshima, T. Komukai, T. Takahashi, N. Norimasa, J. W. J. Wu, R. Moriyama, K. Koyasu and F. Misaizu, *Mass Spectrom.*, 2014, **3**(Spec Iss 3), S0043–S0043.

76 R. Moriyama, R. Sato, M. Nakano, K. Ohshima and F. Misaizu, *J. Phys. Chem. A*, 2017, **121**, 5605–5613.

77 L. A. Angel, L. T. Majors, A. C. Dharmaratne and A. Dass, *ACS Nano*, 2010, **4**, 4691–4700.

78 A. Baksi, A. Ghosh, S. K. Mudedla, P. Chakraborty, S. Bhat, B. Mondal, K. R. Krishnadas, V. Subramanian and T. Pradeep, *J. Phys. Chem. C*, 2017, **121**, 13421–13427.

79 E. Kalenius, S. Malola, M. F. Matus, R. Kazan, T. Bürgi and H. Hakkinen, *J. Am. Chem. Soc.*, 2021, **143**, 1273.

80 S. Malola and H. Hakkinen, *J. Am. Chem. Soc.*, 2019, **141**, 6006.

81 M. Fujii, A. Minami and H. Sugimoto, *Nanoscale*, 2020, **12**, 9266–9271.

82 X. Song, L. Li, H. Qian, N. Fang and J. Ren, *Electrophoresis*, 2006, **27**, 1341–1346.

83 L. Alamo-Nole, S. Bailon-Ruiz, O. Perales-Perez and F. R. Roman, *Anal. Methods*, 2012, **4**, 3127–3132.

84 P. Linkov, P. Samokhvalov, S. Grokhovsky, M. Laronze-Cochard, J. Sapi and I. Nabiev, *Chem. Mater.*, 2020, **32**, 9078–9089.

85 A. N. Beecher, R. A. Dziatko, M. L. Steigerwald, J. S. Owen and A. C. Crowther, *J. Am. Chem. Soc.*, 2016, **138**, 16754–16763.

86 C. K. Manju, D. Ghosh, M. Bodiuzaaman and T. Pradeep, *Dalton Trans.*, 2019, **48**, 8664–8670.

87 C. K. Manju, J. S. Mohanty, D. Sarkar, S. Chennu and T. Pradeep, *J. Mater. Chem. C*, 2018, **6**, 5754–5759.

88 S. Seth and A. Samanta, *J. Phys. Chem. Lett.*, 2018, **9**, 176–183.

89 K. Umemoto, M. Takeda, Y. Tezuka, T. Chiba, M. S. White, T. Inose, T. Yoshida, S. Asakura, S. Toyouchi, H. Uji-i and A. Masuhara, *CrystEngComm*, 2018, **20**, 7053–7057.

90 T. S. Sreeprasad, P. Nguyen, A. Alshogeathri, L. Hibbeler, F. Martinez, N. McNeil and V. Berry, *Sci. Rep.*, 2015, **5**, 9138.

91 S. Kim, S. W. Hwang, M.-K. Kim, D. Y. Shin, D. H. Shin, C. O. Kim, S. B. Yang, J. H. Park, E. Hwang, S.-H. Choi, G. Ko, S. Sim, C. Sone, H. J. Choi, S. Bae and B. H. Hong, *ACS Nano*, 2012, **6**, 8203–8208.

92 W. Wu, J. Cao, M. Zhong, H. Wu, F. Zhang, J. Zhang and S. Guo, *RSC Adv.*, 2019, **9**, 18898–18901.

93 E. Lee, J. Ryu and J. Jang, *Chem. Commun.*, 2013, **49**, 9995–9997.

94 Q. Xue, H. Huang, L. Wang, Z. Chen, M. Wu, Z. Li and D. Pan, *Nanoscale*, 2013, 12098–12103.

95 N. Mohanty, D. Moore, Z. Xu, T. S. Sreeprasad, A. Nagaraja, A. A. Rodriguez and V. Berry, *Nat. Commun.*, 2012, **3**, 844.

96 Q. Hu, X. Gong, L. Liu and M. M. F. Choi, *J. Nanomater.*, 2017, 1804178.

97 C. Rosso, G. Filippini and M. Prato, *ACS Catal.*, 2020, **10**, 8090.

98 F. Rigodanza, M. Burian, F. Arcudi, L. Dordevic, H. Amenitsch and M. Prato, *Nat. Commun.*, 2021, **12**, 2640.

99 L. Dordevic, F. Arcudi, A. D'urso, M. Cacioppo, N. Micali, T. Bürgi, R. Purello and M. Prato, *Nat. Commun.*, 2018, **9**, 3442.

100 T. A. Meyer, Purification Techniques for Three-Dimensional DNA nanostructures, in *3D DNA Nanostructure: Methods and Protocols, Methods in Molecular Biology*, ed. Y. Ke and P. Wang, 2017, ch. 8, vol. 1500.

101 G. B. Salieb-Beugelaar, K. D. Dorfman, A. van den Berg and J. C. T. Eijkel, *Lab Chip*, 2009, **9**, 2508–2523.

102 H.-Q. Wang and Z.-X. Deng, *Chin. Chem. Lett.*, 2015, **26**, 1435–1438.

103 D. Mathur and I. L. Medintz, *Anal. Chem.*, 2017, **89**, 2646–2663.

104 K. Itami and T. Maekawa, *Nano Lett.*, 2020, **20**, 4718–4720.

